BIOCHEMISTRY
including biophysical chemistry & molecular biology
Article

Biochemistry **2010,** *49,* 10277–10286 10277
DOI: 10.1021/bi1014908

Thermodynamics of Cooperative DNA Recognition at a Replication Origin and Transcription Regulatory Site[†]

Mariano Dellarole, Ignacio E. Sánchez,[‡] and Gonzalo de Prat Gay*

Protein Structure−Function and Engineering Laboratory, Fundación Instituto Leloir and IIBBA-Conicet, Patricias Argentinas 435 (1405), Buenos Aires, Argentina. [‡]*Present address: Protein Physiology Laboratory, Departamento de Química Biológica, Facultad de Ciencias Exactas y Naturales, Universidad de Buenos Aires, Buenos Aires, Argentina.*

Received September 14, 2010; Revised Manuscript Received October 29, 2010

ABSTRACT: Binding cooperativity guides the formation of protein−nucleic acid complexes, in particular those that are highly regulated such as replication origins and transcription sites. Using the DNA binding domain of the origin binding and transcriptional regulator protein E2 from human papillomavirus type 16 as model, and through isothermal titration calorimetry analysis, we determined a positive, entropy-driven cooperativity upon binding of the protein to its cognate tandem double E2 site. This cooperativity is associated with a change in DNA structure, where the overall B conformation is maintained. Two homologous E2 domains, those of HPV18 and HPV11, showed that the enthalpic−entropic components of the reaction and DNA deformation can diverge. Because the DNA binding helix is almost identical in the three domains, the differences must lie dispersed throughout this unique dimeric β-barrel fold. This is in surprising agreement with previous results for this domain, which revealed a strong coupling between global dynamics and DNA recognition.

Eukaryotic DNA replication begins with the recognition of defined sequences termed the origin (*ori*) by origin-binding proteins (OBPs).[1] These defined sequences are often tandem repeats of a specific binding site. After binding, OBPs recruit most often hexameric helicases and other proteins, leading to the activation of cellular DNA synthesis machinery. The initiation of replication usually represses transcription (*1*) to prevent the collision of the two machineries (*2*).

Viruses are the smallest self-replicating entities, with small yet complex genomes that encode many functions. Because eukaryotic viral transcription and replication rely heavily on the host machineries and share common mechanisms with host cells, the study of viral molecular genetics has yielded many insights into transcription and replication of eukaryotic genomes (*3*, *4*). *ori* recognition by an OBP is essential for genome replication in double-stranded DNA viruses. This function is fulfilled by the Large T antigen in SV40 (*5*). LANA1 is the counterpart in Kaposi's sarcoma-associated herpesvirus (*6*) and EBNA1 in Epstein-Barr virus (*7*), and the E1 and E2 proteins are the counterparts in papillomaviruses (*8*). In most cases, binding of the OBP to its target DNA sequence is actively involved in the regulation of viral transcription (*7*, *9*−*11*) and chromosomal segregation (*6*, *12*−*14*).

Most DNA tumor viruses bear multiple copies of the OBP target DNA sequence at the origin of replication (*12*, *15*−*18*). Cooperative binding (*19*) of regulatory proteins to these multiple target sequences is essential for the precise and economical regulation of the recruitment of the transcription and/or replication machineries (*20*). In vitro experiments such as electrophoretic mobility shift assays showed in all cases tested that binding to multiple target sequences at viral origins of replication takes place with positive cooperativity (*15*, *21*−*25*). The thermodynamic and structural changes that accompany cooperative protein−DNA binding are key to the recognition, bending, and unwinding of DNA sites during transcription and replication but are still poorly understood.

Human papillomavirus (HPV) types that infect mucosal epithelia are highly infectious pathogens causing a variety of lesions that go from innocuous to malignant, where the most widespread is cervical cancer (*26*). Of the more than 100 types of HPV, there are more than 50 mucosal HPV types, all of them belonging to the alpha genus (*27*). Types 11 (low cancer risk) and types 16 and 18 (high cancer risk) are among the most prevalent and therefore are used as model systems for papillomavirus research. The noncoding upstream regulatory region (URR) of the HPV genome is ~900 bp long and contains the target DNA sequences for the HPV E1 and E2 proteins (Figure 1A). Binding of E2 to its adjacent binding sites BS1 and BS2 proximal to the transcription start and *ori* sites is fundamental for the recruitment of E1 helicase, which in turn unwinds the origin of replication and recruits the host replication machinery (*8*, *28*, *29*). E2 also regulates the expression of viral proteins: binding to tandem sites BS1 and BS2 (double binding site, DBS) leads to repression of oncogene transcription by steric displacement of Sp1

[†]This work was supported by a Wellcome Trust Grant (GR077355AYA), the Agencia Nacional de Promoción Científica y Tecnológica PICT (2000 01-08959), a doctoral fellowship from Consejo Nacional de Investigaciones Científicas y Técnicas to M.D., and a postdoctoral fellowship from Consejo Nacional de Investigaciones Científicas y Técnicas to I.E.S. G.d.P.G. is a Career Investigator from Consejo Nacional de Investigaciones Científicas y Técnicas.

*To whom correspondence should be addressed. E-mail: gpg@leloir.org.ar. Phone: +54 11 5238 7500, ext. 3209. Fax: +54 11 5238 7501.

[1]Abbreviations: HPV, human papillomavirus; *ori*, replication origin; OBP, origin-binding protein; E2C, E2 DNA binding domain; BS, DNA binding site; DBS, DNA double binding site; ITC, isothermal titration calorimetry; CD, circular dichroism; PDB, Protein Data Bank.

Published on Web 11/03/2010

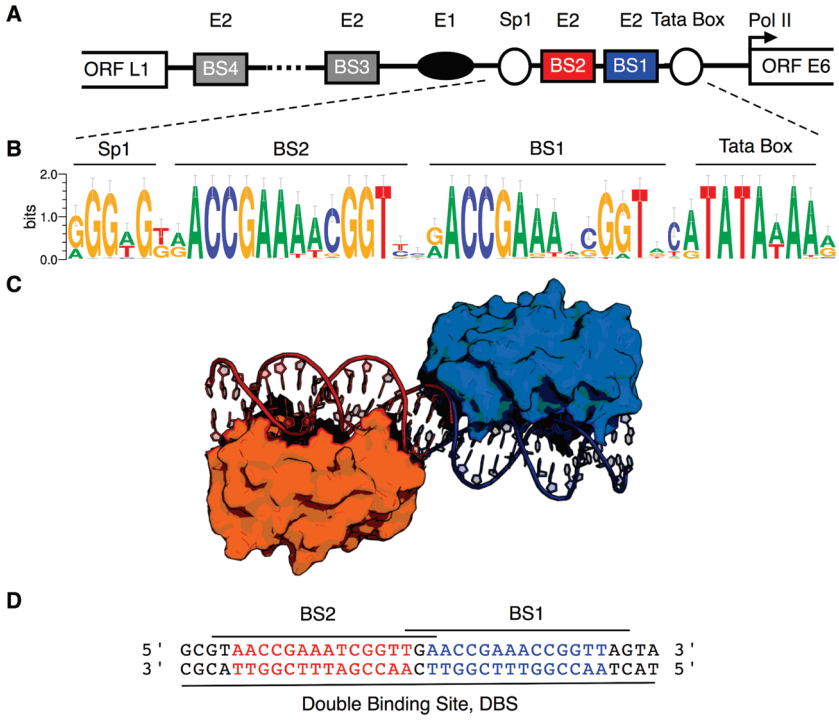

FIGURE 1: E2 binding sites in the alpha papillomavirus upstream regulatory region. (A) Schematic view of the upstream regulatory region of a prototypical alpha papillomavirus genome. Shown are flanking ORFs L1 and E6, E2 binding sites BS1, BS2, BS3, and BS4, the E1 binding site, the Sp1 binding site, and the TATA box. (B) Sequence logo (*57*, *58*) of the cis-responsive elements of the E6 promoter. (C) Model of the complex of two E2C homodimers with two adjacent sites separated by one base. Under our experimental conditions, E2C is always dimeric. The model was constructed by aligning two copies of a HPV6 E2C−DNA complex (PDB entry 2ayg) using PyMol (Delano Scientific LLC). (D) Sequence of the double-stranded oligonucleotide DBS from HPV16, with BS1 colored blue and BS2 red.

and TATA binding protein (TBP) from their binding sites (Figure 1A) (*30*−*32*). Binding of E2 to the more distant BS4 activates viral transcription and DNA looping between BS4 and DBS (*33*−*35*). The sequence and relative positions of E2, Sp1, and TBP binding sites are highly conserved in the alpha genus (*18*) (Figure 1B), underscoring the importance of this region and of the DBS in the life cycle of the virus. Because the switch between replication and transcription in HPV is spatially and temporally regulated by the E2 protein along the virus life cycle, E2 is considered as a master regulator.

The E2 protein is highly conserved among papillomavirus and consists of an ~400-amino acid chain, with an N-terminal transactivation domain, a C-terminal dimeric DNA binding domain (E2C), and a flexible "hinge domain" (*36*). E2C is a homodimeric β-barrel protein (*36*−*41*), which binds to a highly conserved pseudopalindromic target site (Figure 1B). Interestingly, this unique fold has been found only in the DNA binding domain of Epstein-Barr nuclear antigen 1 (EBNA1), which acts as an OBP, but with otherwise no amino acid or DNA site sequence homology (*42*). The structure of the EBNA1 DNA binding domain bound to its target DNA was modeled on two adjacent sites, and it was proposed that a 20° unwinding in the DNA was required to explain the positive cooperativity, although no quantitative analysis was conducted (*25*, *43*). When bound to E2, the target DNA is in the B form and presents a global bend angle of 24−43°, as revealed by the structures of HPV18 and HPV6 E2C domains with DNA (*44*, *45*).

We have been using HPV16 E2C as a model for folding and protein−DNA interaction mechanisms (*36*). Detailed mapping of the binding interface allowed us to determine that all individual side chain−base interactions are additive as opposed to cooperative in energetic terms, with none of the interface interactions acting as a "hot spot" as frequently found in protein−protein interfaces (*46*). Formation of the complex between HPV16 E2C and BS2 can take place via two alternative kinetic routes (*47*−*49*). One of them can be described as two-state, while the other populates at least two intermediates (*48*, *49*); we were able to describe a DNA−protein interaction landscape for each of the routes (*48*, *49*). In addition, we determined that recognition of DNA by E2C is an enthalpically driven process (*50*−*52*). More recently, we showed that specific recognition of DNA by E2C implies a coupling among histidine protonation, global structural cooperativity, and dynamics, through an "indirect readout" effect on the protein side (*52*).

Using the binding of E2C to its tandem double-site cognate sequence as a model, we set out to investigate the thermodynamic basis for the cooperative recognition of this viral replication origin as a model for replication initiation and transcription repression, and in particular for DNA tumor virus tandem site origins. In addition, we intended to address conformational changes in the DNA that must take place for DNA replication to start. We determined the thermodynamic basis for binding cooperativity using isothermal titration calorimetry (ITC), a challenging task considering the complexity of the system, and correlated it most likely to partial local unstacking (*53*). Given the possibility of different but highly related HPV E2C domains, we compared binding of E2C domains from HPV11, HPV16, and HPV18 (E2C-11, E2C-16, and E2C-18) to individual single sites and the double site from the HPV16 genome. This allowed us to test for the consequences of sequence divergence among representative viral types on binding cooperativity. Besides a model system, gene expression and replication control in HPV are essential for cancer progression and a pursued antiviral target.

EXPERIMENTAL PROCEDURES

Proteins. E2C-11 and E2C-18 were recombinantly expressed, purified, and stored as previously described for E2C-16 (*54*). The molecular weight and purity of recombinant proteins were tested by matrix-assisted laser desorption ionization (MALDI) and by sodium dodecyl sulfate−polyacrylamide gel electrophoresis (SDS−PAGE). Protein concentrations were determined spectroscopically using the molar extinction coefficients (ε_{280}): 30940, 41940, and 33920 μM^{-1} cm^{-1} for E2C-11, E2C-16, and E2C-18, respectively. The three domains are known to form homodimers in solution with subnanomolar dissociation constants (*44*, *55*, *56*). Thus, the concentration of E2C monomers in our experiments can be considered negligible.

DNA. Oligonucleotides were purchased from Integrated DNA Technologies (Coralville, IA). Sequences are shown in Figure 1D. We performed annealing by mixing equal amounts of the oligos in 10 mM BisTris buffer (pH 7.0) and 50 mM NaCl, incubating the mixture for 5 min at 95 °C, and slowly cooling the mixture to 25 °C over 16 h. This yielded a double-stranded oligonucleotide. No detectable single-stranded oligonucleotide was present as judged by 20% polyacrylamide gel electrophoresis. The double-stranded oligonucleotide concentration was calculated using molar extinction coefficients (ε_{260}) obtained from the nucleotide composition of 369300, 352400, and 715100 μM^{-1} cm^{-1} for BS1, BS2, and DBS, respectively.

Sequence Logo. Sequence logos were generated with WebLogo (*57*, *58*) and the aligned DNA. All alpha papillomavirus genomes were obtained from the International Committee on Taxonomy of Viruses data Base (*59*) (taxonomy ID 151340) and manipulated as described previously (*18*). We used the alignment editors BioEdit version 7.0.8 (T. Hall, Ibis Biosciences) and Jalview version 2.2.1 (*60*) for sequence manipulation. Nucleotide positions with a proportion of ≥60% gaps were removed for the sake of clarity.

Isothermal Titration Calorimetry (*ITC*). Proteins and DNA were extensively dialyzed at 4 °C against the measurement buffer prior to the experiment. Binding experiments were performed using the VP-ITC calorimeter (MicroCal). The volume of each injection was 8 or 10 μL, except that of the first injection, which was 2 μL. Syringe rotation was fixed to 290 rpm. Titrations were continued beyond saturation levels to allow for determination of heats of ligand dilution. ORIGIN version 5.0, supplied with the calorimeter, was used to subtract the heat of dilution. Measurements were performed in the presence of 200 mM phosphate so that the binding constants could be determined from the ITC measurements (*51*, *61*).

Binary Complexes. BS1 or BS2 at concentrations in the range of 80−100 μM was titrated into the ITC cell containing 8−10 μM E2C. Global fits to a single-site binding model of data obtained from at least two titrations for each site were conducted using SEDPHAT (*62*).

Ternary Complexes. In "direct" titrations of the ternary complex, DBS at concentrations in the range of 32.9−40.5 μM was titrated into the ITC cell containing 4.5−4.9 μM E2C. In reverse titrations of the ternary complex, E2C at concentrations in the range of 41.2−48.1 μM was titrated into the ITC cell containing 3.3−4.4 μM DBS. Global fits to a two-site binding model of data obtained from direct and reverse titrations of each ternary complex were conducted using SEDPHAT (*62*).

Spectroscopy. Circular dichroism and absorbance spectra were recorded in a Jasco (Japan) J815 instrument in a 0.1 cm path length cuvette. All complexes were studied at a concentration of 15 μM. All complexes were incubated for 30 min at 298.15 K and centrifuged for 15 min at 13000 rpm before measurement. Ten scans were accumulated and averaged for each measurement. The spectrum of the buffer was recorded and subtracted from all sample spectra. Data analysis was performed in pro Fit (Quantum Soft).

Kinetics. Kinetics of structural changes were recorded in an Applied Photophysics SX18-MV spectrophotometer. Absorbance was measured at 270 nm (4 nm slit). One volume of 2 μM DNA was mixed with 1 volume of protein to yield final protein:DNA stoichiometries of 2:1, 4:1, and 8:1.

Population Analysis. Fractional populations of free DBS, DBS bound to a single E2C domain, and the ternary complex were calculated as a function of E2C concentration using the measured values for K_{BS1}, K_{BS2}, and K_{coop} as follows:

$$\text{fraction free DBS} = 1/(1 + K_{BS1}[\text{E2C}] + K_{BS2}[\text{E2C}] + K_{BS1}K_{BS2}K_{coop}[\text{E2C}]^2) \quad (1)$$

$$\text{fraction one site bound} = (K_{BS1}[\text{E2C}] + K_{BS2}[\text{E2C}])/(1 + K_{BS1}[\text{E2C}] + K_{BS2}[\text{E2C}] + K_{BS1}K_{BS2}K_{coop}[\text{E2C}]^2) \quad (2)$$

$$\text{fraction two sites bound} = (K_{BS1}K_{BS2}K_{coop}[\text{E2C}]^2)/(1 + K_{BS1}[\text{E2C}] + K_{BS2}[\text{E2C}] + K_{BS1}K_{BS2}K_{coop}[\text{E2C}]^2) \quad (3)$$

RESULTS

Binding Model and Considerations. The first step in investigating the cooperative recognition of the HPV origin used as a model is to determine the thermodynamic basis for the recognition of the separate cognate DNA binding sites BS1 and BS2 that are configured in tandem in the HPV genome (DBS) to two E2C homodimers (Figure 1). We make use of a general binding model (Scheme 1) (*21*)in which E2C:DBS_1 denotes binding of an E2C homodimer to BS1 within DBS to form a binary complex, with an equilibrium constant K_{BS1}, and E2C:DBS_2 denotes binding of an E2C dimer to BS2 within DBS to form a binary complex, with an equilibrium constant K_{BS2}. The presence of flanking nonspecific DNA does not affect E2C binding (*49*). Finally, E2C:DBS:E2C denotes binding of two E2C homodimers to DBS to form a ternary complex, with an equilibrium constant $K_{BS1}K_{BS2}K_{coop}$. The cooperativity constant K_{coop} is 1 for independent binding of the two E2C homodimers. A K_{coop} of >1 implies positive cooperativity; that is, binding of the second E2C molecule is favored when an E2C molecule is already bound to DBS (*19*). A K_{coop} of <1 implies negative cooperativity; that is, binding of the second E2C molecule is disfavored when an E2C molecule is already bound to DBS (*21*).

For the sake of clarity, we have built an informative scheme of the ternary complex between DBS and two E2C molecules

Scheme 1

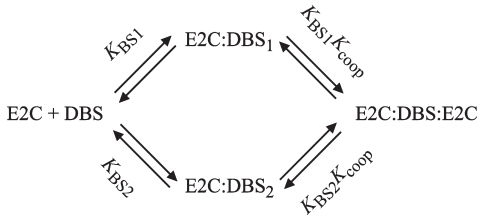

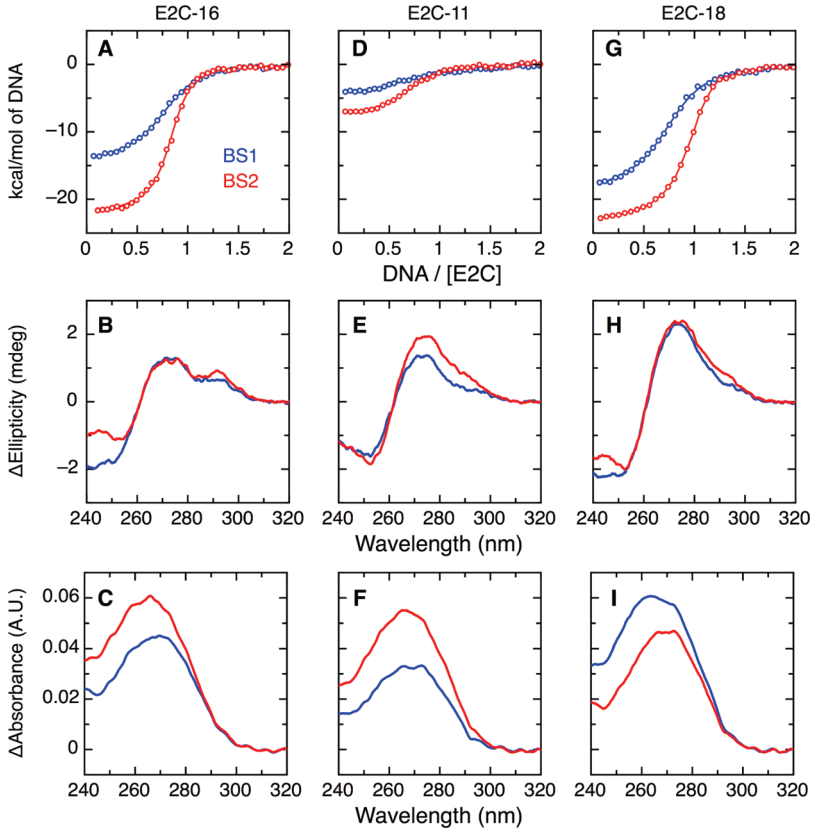

FIGURE 2: Binding of E2C to BS1 and BS2. Experiments were performed in 200 mM sodium phosphate (pH 7) and 0.2 mM DTT at 298 K. The top panels show integrated, concentration-normalized binding isotherms of BS1 (blue) or BS2 (red) injected into the ITC cell containing protein. The solid lines represent global fits (*62*) to a single-site binding model of data points of at least two independent experiments for each homologous protein: (A) E2C-16, (D) E2C-11, and (G) E2C-18. The middle panels show difference CD spectra for binding of E2C to BS1 (blue) and BS2 (red): (B) E2C-16, (E) E2C-11, and (H) E2C-18. The spectra of E2C and BS1 or BS2 were subtracted from the spectra of each 1:1 E2C complex. All data are shown to the same scale for direct comparison. The bottom panels show difference absorbance spectra for binding of E2C to BS1 (blue) and BS2 (red): (C) E2C-16, (F) E2C-11, and (I) E2C-18. The spectra of E2C and BS1 or BS2 were subtracted from the spectra of each 1:1 E2C complex.

(Figure 1C) by manually superimposing the most distal bases of two E2C−DNA complexes so that the distance between BS1 and BS2 is one base, as in the HPV16 genome (Figure 1D). Albeit rough, this approximation clearly shows that independent bending to the two sites would position the two E2C molecules at opposite sides of the DNA. Thus, on the basis of this model, additive binding of E2C to DBS can in principle be expected in the HPV16 genome, and protein−protein contacts seem unlikely. This work aims to answer these questions in mechanistic and thermodynamic terms.

Binding of E2C to Isolated BS1 and BS2. We conducted the analysis of the cognate interaction between E2C-16 and DBS (Figure 1D). Throughout this work, all experiments were performed in 200 mM sodium phosphate (pH 7) and 0.2 mM DTT at 298 K. To determine all binding constants in Scheme 1 with reliability, we first investigated binding of E2C-16 to the isolated sites BS1 and BS2 (Figure 1D) by ITC. Figure 2 shows integrated, concentration-normalized data for injection of BS1 (blue circles) or BS2 (red circles) into the cell containing E2C-16 (Figure 2A). The observed reaction stoichiometry is ≥0.8, and the *c* value is >10 (Table 1), validating fitting a 1:1 binding model to the data. The fit yields the binding free energies (ΔG) and their enthalpic and entropic components (Table 1). Binding of E2C-16 to the individual cognate sites was enthalpy-driven in both cases, where binding to BS2 was significantly stronger than binding to BS1 (4-fold difference in the equilibrium binding constant, *K*).

Formation of E2C−DNA complexes induces bending of the DNA toward the minor groove and small rearrangements in the protein, as indicated by crystallographic evidence (*44*, *45*) and solution measurements (*38*, *54*). Because of the large difference in extinction coefficients in favor of DNA, the contribution of the protein to the spectra is minor and easily subtractable in absorbance and negligible in near-UV CD, which allows us to determine that spectral changes correspond mostly to DNA conformation (*53*, *63*). Thus, we may attribute the changes in CD and absorbance spectra to DNA bending and torsion. We recorded spectra of isolated DNA sites, E2C-16, and the 1:1 protein−DNA complexes. The CD spectra of free and bound BS1 and BS2 show a positive peak at 275 nm, a crossover at 260 nm, and a negative peak at 245 nm (Figure S1 of the Supporting Information), characteristic of B-form DNA (*53*, *63*, *64*), as expected from structural data (*44*, *45*). We calculated difference CD and absorbance spectra by subtracting the individual spectra of the free DNA and protein from the spectra of the corresponding complexes. The difference spectra represent the combined spectral changes mainly in DNA upon binding. As expected from previous results (*38*, *44*, *45*, *54*), we observed an increase in both the magnitude of the CD signal at 275 nm (Figure 2B) and the absorbance at 265 nm (Figure 2C) for the binary complex of E2C-16 with either BS1 or BS2.

As stated above, the possibility of evaluating E2C domains from related HPV types not only provides insight into the different mechanisms among the types related to the virus biology but also more importantly allows us to compare a differential behavior related to our reference data on HPV16 E2C with

Table 1: Thermodynamics of Binding of E2C to BS1 and BS2

DNA	parameter	E2C-16	E2C-11	E2C-18
BS1	K_{BS1} (M^{-1})	$(4.0 \pm 0.5) \times 10^6$	$(1.7 \pm 0.6) \times 10^6$	$(2.5 \pm 0.1) \times 10^6$
	ΔG (kcal/mol)	-9.0 ± 0.1	-8.5 ± 0.2	-8.7 ± 0.1
	ΔH (kcal/mol)	-15.2 ± 0.4	-5.8 ± 0.7	-19.5 ± 0.9
	$-T\Delta S$ (kcal/mol)	6.2 ± 0.3	-2.7 ± 0.5	10.8 ± 0.8
	N^a	0.8 ± 0.1	0.8 ± 0.1	0.8 ± 0.1
	c value^b	28 ± 5	11 ± 3	21 ± 1
BS2	K_{BS2} (M^{-1})	$(1.1 \pm 0.4) \times 10^7$	$(4.6 \pm 0.7) \times 10^6$	$(7.9 \pm 0.3) \times 10^6$
	ΔG (kcal/mol)	-9.6 ± 0.2	-9.1 ± 0.1	-9.4 ± 0.1
	ΔH (kcal/mol)	-22.7 ± 0.4	-7.9 ± 0.1	-24.1 ± 0.3
	$-T\Delta S$ (kcal/mol)	13.1 ± 0.2	-1.2 ± 0.1	14.7 ± 0.3
	N^a	0.8 ± 0.1	0.9 ± 0.1	0.9 ± 0.1
	c value^b	82 ± 29	29 ± 2	64 ± 5

[a]Stoichiometry of the reaction calculated from the incompetent fraction of the ligand (*62*). [b]Ratio of the ligand concentration to the product of the dissociation constant and the measured stoichiometry (*61*). Errors were derived from the standard deviation of at least two single experiments.

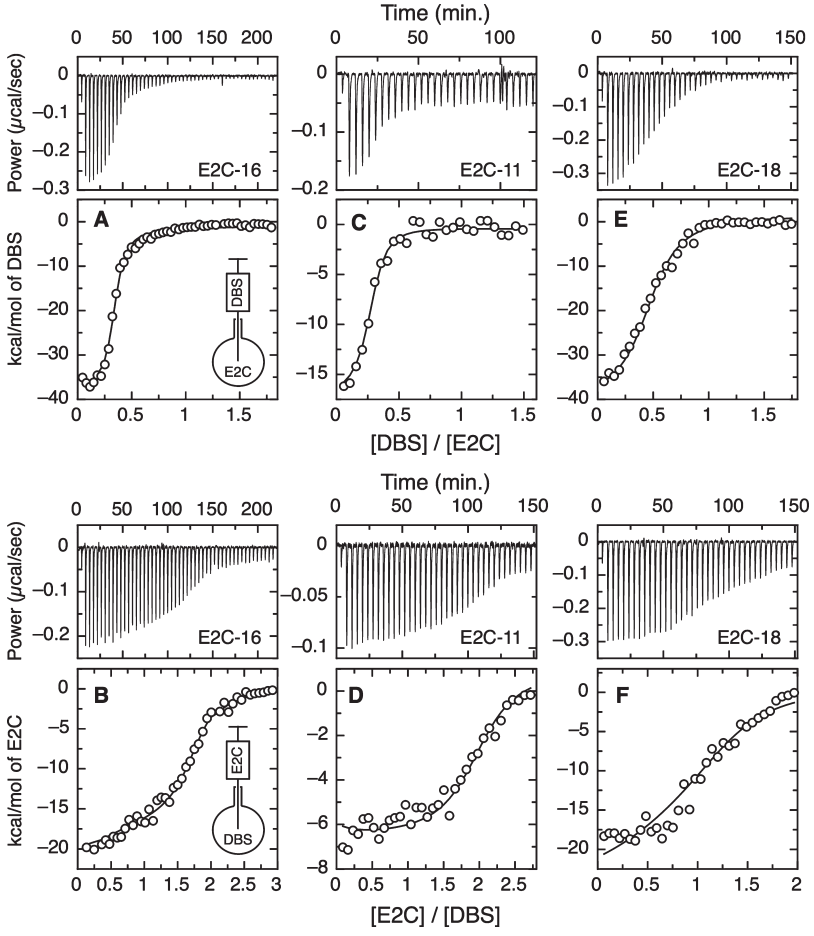

FIGURE 3: Binding of E2C to the tandem DNA site DBS. Experiments were performed in 200 mM sodium phosphate (pH 7) and 0.2 mM DTT at 298 K. Each panel shows the ITC data in both raw and integrated, concentration-normalized form. The top panels show direct ITC titrations, i.e., injecting DBS into a cell containing E2C: (A) E2C-16, (C) E2C-11, and (E) E2C-18. The bottom panels show reverse ITC titrations, i.e., injecting E2C into a cell containing DBS: (B) E2C-16, (D) E2C-11, and (F) E2C-18. Lines are global fits (*62*) to the two-site binding model of direct and reverse titrations for each homologous protein.

evolutionarily related variants of the domain. Binding of E2C-11 (Figure 2D) and E2C-18 (Figure 2G) to BS1 and BS2 is also enthalpy-driven, and binding to BS2 is significantly stronger than binding to BS1, as in the case of HPV16 (Table 1). This feature is in agreement with our previous proposal that sequence specificity is conserved across E2C domains from alpha papillomaviruses (*18*). There are differences in enthalpic and entropic contributions to binding energy among the three proteins that merit further detailed investigation with more HPV-type variants. Binding of E2C-11 and E2C-18 to BS1 and BS2 followed by CD (Figure 2E,H) and absorbance (Figure 2F,I) leads to spectroscopic changes comparable to those observed for E2C-16. This indicates that the conformational changes in solution that take place in BS1 and BS2 upon binding of the three domains are similar, in agreement with previously reported crystallographic data for E2C-18 (*44*) and E2C-6 (*45*).

Thermodynamics of Binding of E2C to the Tandem DNA Site DBS. Binding of E2C-16 to the tandem DBS was investigated by

ITC (Figure 1C). Figure 3A shows the experiment conducted by direct titration, i.e., injecting DNA into a cell containing the protein. In the first injections, the large excess of protein leads to predominant formation of the ternary E2C−DBS−E2C complex. The apparent DNA:protein stoichiometry, N_{direct}, is on the order of 1:2, and the apparent enthalpy of binding (Figure 3A, approximately −38 kcal/mol) is close to the sum of the ΔH values for binding to isolated BS1 and BS2 (see Table 1). Figure 3B shows the experiment conducted by reverse titration, i.e., injecting protein into a cell containing DNA. As expected for a multisite system, the observed shape of the isotherms depends on the order of addition in the titration experiment (see Figure S2 of the Supporting Information for an explicative scheme). In the first injections, the large excess of DNA leads to predominant formation of the binary E2C−DBS_1 and E2C−DBS_2 complexes. The apparent protein:DNA stoichiometry $N_{reverse}$ is on the order of 2:1, and the apparent enthalpy of binding is close to the average of the ΔH values for binding to isolated BS1 and BS2 (compare the ΔH of −20 kcal/mol from Figure 3B with data from Table 1).

Table 2: Thermodynamics of Binding of E2C to the Tandem DNA Site DBS

parameter	E2C-16	E2C-11	E2C-18
N_{direct} [a]	0.4 ± 0.1	0.3 ± 0.2	0.5 ± 0.1
$N_{reverse}$ [b]	1.6 ± 0.1	1.9 ± 0.1	1.3 ± 0.1
K_{coop}	2.6 ± 0.3	3.4 ± 0.8	0.8 ± 0.2
ΔG_{coop} (kcal/mol)	−0.6 ± 0.1	−0.7 ± 0.1	0.1 ± 0.1
ΔH_{coop} (kcal/mol)	0.9 ± 0.5	−3.1 ± 0.5	2.3 ± 1.1
$-T\Delta S_{coop}$ (kcal/mol)	−1.5 ± 0.5	2.3 ± 0.6	−2.1 ± 1.2

[a]Stoichiometry of the reaction for direct titration, i.e., injecting DNA into a cell containing protein. [b]Stoichiometry of the reaction for reverse titration, i.e., injecting protein into a cell containing DNA. Stoichiometries were calculated from the incompetent fraction of ligand (*62*). Errors were derived from Monte Carlo analysis of global fits (*62*).

We have globally fitted (*62*) the binding model shown in Scheme 1 to the direct and reverse titrations (see Experimental Procedures). The binding constants and enthalpies of binding of E2C-16 to BS1 and BS2 within DBS were held constant during fitting to the values measured for the isolated sites (Table 1). The fit yields parameters for the cooperativity constant K_{coop} (and, thus, the free energy of cooperativity ΔG_{coop}) and its enthalpic and entropic components (Table 2). The binding model (Scheme 1) fit the data very well (Figure 3A,B), and the observed stoichiometry is close to the expected value (Table 2), thus validating our approach. We confirmed direct and reverse stoichiometries using fluorescence and anisotropy titrations and electrophoresis mobility shift assays (Figure S3 of the Supporting Information). E2C-16 binds to its cognate tandem DNA site DBS with positive cooperativity [K_{coop} = 2.6 ± 0.3 (Table 2) (ΔG_{coop} = −0.6 ± 0.1 kcal/mol)]. Fitting a model with two nonidentical independent sites (K_{coop} = 1) to the data resulted in a 2-fold higher χ^2 value (Figure S4 of the Supporting Information), confirming that the formation of the ternary complex is cooperative. The dissection of ΔG_{coop} into its enthalpic and entropic components is shown in Figure 4A. Interestingly, positive cooperativity is governed by entropy for E2C-16, with a $-T\Delta S_{coop}$ of −1.5 ± 0.5 kcal/mol (Table 2).

Binding of E2C-11 to DBS shows a K_{coop} of 3.4 ± 0.8 (Table 2) (ΔG_{coop} = −0.7 ± 0.1 kcal/mol), similar to that of E2C-16. However, the positive cooperativity of E2C-11 bears an enthalpic origin, with a ΔH_{coop} of −3.1 ± 0.5 kcal/mol (Figure 4C). E2C-18 binds to the tandem DNA site DBS in a noncooperative manner with a K_{coop} of 0.8 ± 0.2 (ΔG_{coop} = 0.1 ± 0.1 kcal/mol). The χ^2 value is only slightly improved by inclusion of cooperativity in the binding model (Figure S4 of the Supporting Information). Surprisingly, the near-zero ΔG_{coop} for E2C-18 originates in compensating enthalpic and entropic contributions, which are similar in magnitude to those observed for E2C-11 and E2C-16 (Figure 4E).

We illustrate the consequences of binding cooperativity by simulating the fractional population of free DBS, DBS with one

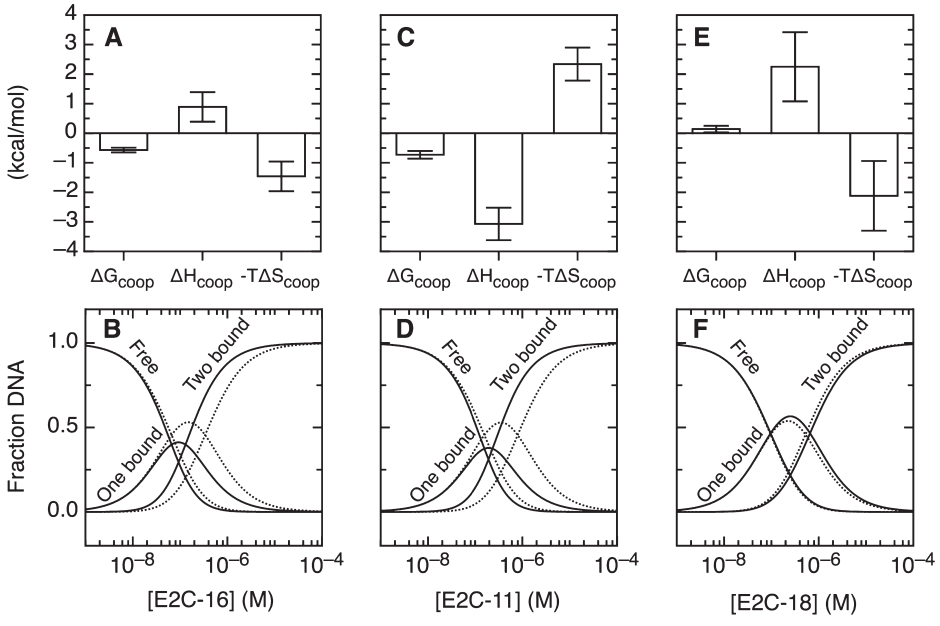

FIGURE 4: Cooperative binding of E2C to the tandem site DBS. The top panels show thermodynamic dissection of (A) E2C-16, (C) E2C-11, or (E) E2C-18 binding to DBS. Negative values represent a favorable additional contribution to binding, whereas positive values represent an unfavorable additional contribution to binding. The bottom panels show the fractional population of free DBS, DBS with one site occupied, and DBS with both sites occupied as a function of (B) E2C-16, (D) E2C-11, or (F) E2C-18 concentration. Solid lines were calculated using the measured values of K_{BS1}, K_{BS2}, and K_{coop}. Dotted lines were calculated using the measured values of K_{BS1}, K_{BS2}, and K_{coop} set to 1.

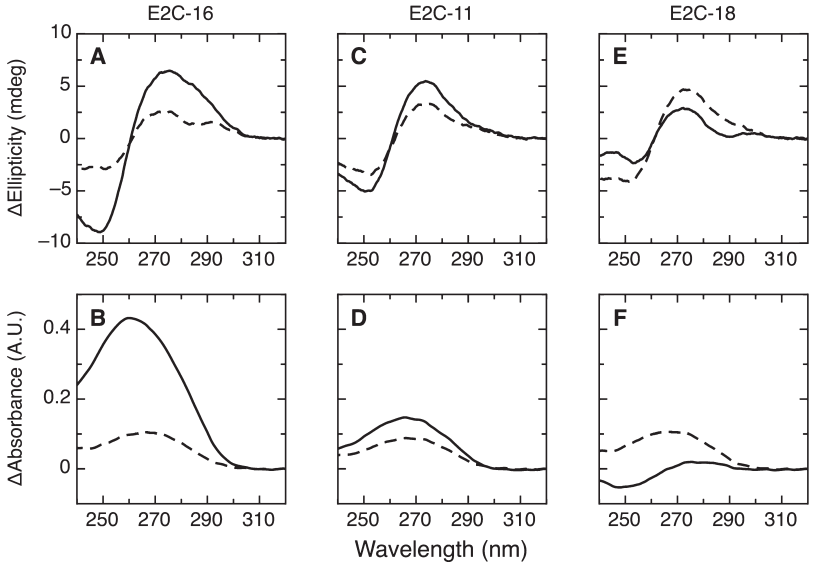

FIGURE 5: Spectroscopic changes associated with binding of E2C to the tandem DNA site DBS. Experiments were performed in 200 mM sodium phosphate (pH 7) and 0.2 mM DTT at 298 K. Solid lines are difference spectra for binding of E2C to DBS. The spectra of DBS and two E2C molecules were subtracted from the spectra of the E2C−DBS−E2C ternary complex. Dashed lines are sums of difference spectra for the E2C−BS1 and E2C−BS2 complexes. The top panels show difference CD spectra: (A) E2C-16, (C) E2C-11, and (E) E2C-18. The bottom panels show difference absorbance spectra: (B) E2C-16, (D) E2C-11, and (F) E2C-18.

site occupied, and DBS with both sites occupied (Figure 4, bottom panels) (see Experimental Procedures). Solid lines were calculated using the measured values of K_{BS1}, K_{BS2}, and K_{coop}, and dashed lines were calculated using the measured values of K_{BS1}, K_{BS2}, with K_{coop} set to 1. Positive binding cooperativity for E2C-16 and E2C-11 has two linked effects (Figure 4B,D). Relative to additive binding, the ternary complex is populated at lower E2C concentrations and the binary complexes are populated to a lesser degree.

DNA Conformational Changes Associated with Binding of E2C to DBS. We used CD and absorbance spectroscopy as reporters of changes in the DNA conformation of DBS upon formation of the cognate ternary complex with E2C-16 and compared them to those associated with individual single-site binding. We recorded spectra for the isolated DBS and for the ternary E2C−DBS−E2C complex. The CD spectra of the free DBS and of the ternary complex exhibit a positive peak at 275 nm, a crossover at 260, and a negative peak at 245 nm (Figure S5 of the Supporting Information), characteristic of B-form DNA (*53*, *63*, *64*). This shows that the DNA of DBS forms a B type of helix both in its free form and in the ternary complex with E2C-16.

We obtained difference CD and absorbance spectra for the ternary complex by subtracting the spectra of DBS and of E2C-16 (in a 1:2 molar ratio) from the spectra of the E2C−DBS−E2C complex. These difference spectra represent the combined CD and absorbance changes in DBS DNA upon binding (solid lines in Figure 5A,B). We then compared the difference spectra (both CD and absorbance) for the ternary complex with the sum of difference spectra for each individual E2C−BS1 and E2C−BS2 binary complex (dashed lines in Figure 5A,B). Interestingly, there are evident differences between the two spectra, indicating that formation of the ternary complex involves a conformational rearrangement in DBS DNA that goes beyond those observed for single-site binding (Figure 2B,C).

We have also calculated the respective difference spectra for the ternary complexes of DBS with E2C-11 and E2C-18 (solid lines in Figure 5C−F) and the sum of difference spectra for the binary complexes of E2C-11 and E2C-18 with BS1 and BS2 (dashed lines in Figure 5C−F). The considerable differences between the solid and dashed lines for both E2C-11 and E2C-18 show that, as in the case of E2C-16, formation of the ternary complexes involves conformational rearrangements in DBS, in addition to the ones observed for single-site binding. Remarkably, the difference between the conformation of DBS (solid lines) and the sum of individual sites BS1 and BS2 (dashed lines) varies among the three E2C domains. This suggests that the structural changes in DBS associated with formation of the ternary complex depend on the E2C domain variant.

Kinetics of E2C−DBS Interaction: Time-Dependent DNA Structural Changes. Finally, the kinetics of formation of the ternary complex of E2C-16 with DBS was investigated by stopped-flow techniques (see Experimental Procedures). We mixed equal volumes of 2 μM E2C-16 and 1 μM DBS and followed the changes in absorbance. The E2C−DNA association events previously determined by us and others showed a k_{on} of $0.1-1.4 \times 10^9\ M^{-1}\ s^{-1}$ (*45*, *47*). Thus, under these conditions that require high concentrations of the reactants to produce a good signal-to-noise ratio, the two molecules associate within the ~2 ms dead time of the instrument and any further observed signal changes should correspond to unimolecular conformational rearrangements. Under these conditions, the changes in the absorbance signal observed at equilibrium (Figure 5B) indeed occur within the dead time of the instrument (data not shown). Thus, in the case of E2C-16, the DNA conformational rearrangements in DBS take place on the submillisecond time scale, most likely in parallel with the bimolecular association event.

Conversely, changes in DNA conformation upon binding of E2C-11 are observed within the experimental window (Figure 6). The kinetics is described well by a single-exponential function with an observed rate constant of $44.9 \pm 0.5\ s^{-1}$. This rate constant is independent of E2C concentration in the range of 2−8 μM (Figure S6 of the Supporting Information), indicating that the rate-limiting step of the reaction under these conditions is a unimolecular process. Thus, for E2C-11, the ternary complex undergoes an observable conformational transition in DBS after

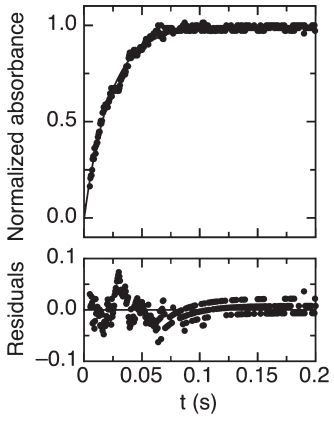

FIGURE 6: Kinetics of structural changes upon binding of E2C to the tandem DNA site DBS. DBS (1 μM) was mixed with 2 μM E2C-11 in 200 mM sodium phosphate (pH 7) and 1 mM DTT at 298 K, and the changes in absorbance at 270 nm were followed. Shown are the normalized data and the fit to a single-exponential function.

the association step, which on the basis of the known association rates, takes place within the experimental dead time (*45*, *47*). We did not observe any changes in absorbance upon binding of E2C-18 to DBS, as expected from the spectra of the complex and the separate components (Figure S6F of the Supporting Information).

DISCUSSION

To complement the structure and biology of eukaryotic DNA origin replication sites, and in particular those of tumor DNA viruses, we undertook a thermodynamic and conformational dissection of the complex between the DNA recognition domain of the master regulator protein, E2, and two DNA sites arranged in tandem at the *ori* and cis-regulatory region of HPV type 16 (Figure 1). The thermodynamic analysis of data for the formation of ternary complexes by ITC is a challenging task (refs *65* and *66* and reviewed in ref *67*), especially so in the case of protein−DNA interaction where it is common in the literature to find incomplete cooperative ITC analysis (e.g., refs *68* and *69*). The usual technical strategies for addressing cooperative protein−DNA recognition are EMSA (e.g., ref *21*) and fluorescence spectroscopic assays (e.g., refs *70* and *71*). However, our binding system presents a scenario in which recognition of isolated DNA sites is not equivalent (Figure 2) and binding to tandem sites is not independent (Figure 3), increasing the degree of complexity. To address the cooperative interaction of E2C and DBS, we started by using EMSA and fluorescence spectroscopy, but we could not interpret the population of the species involved beyond the verification of the stoichiometry (Figure S3 of the Supporting Information), because of the intricate nature of the binding model. Because the quantitative discrimination of the individual complexes is not possible on the basis of the fluorescence signal, we concentrated on the ITC data.

The fact that we could measure the enthalpies of each individual process independently and accurately (Figure 2) allowed us to tackle the binding analysis of the ternary E2C−DBS−E2C complex by ITC. We first measured binding to the isolated sites BS1 and BS2 separately (Figure 2) and subsequently global fitting of direct and reverse titrations of the tandem site (Figure 3) (*62*). Our data for E2C-16 produce the best fit with a cooperativity constant of 2.6 ± 0.3 (Table 2). This value is in line with the low cooperativity constant of 1.7 measured earlier via an EMSA (*21*). However, modeling of the EMSA data involves a larger error and assumed that the affinity of E2C for BS1 and BS2 was the same (*21*), which was shown to be incorrect (Figure 2, Table 1, and ref *72*).

Formation of the binary complexes of BS1 and BS2 with E2C-16 is associated with small changes in the CD signal at 275 nm of approximately 1 mdeg and changes of 0.04−0.06 absorbance unit at 270 nm (Figure 2), in agreement with previous results (*38*, *54*). The spectral changes upon binding of E2C domains to DBS differ from those expected in the case of independent binding by ~4 mdeg at 275 nm for CD and ~0.3 absorbance unit at 270 nm (Figure 5). We hypothesize that the additional structural changes in DBS associated with binding of E2C-16 are larger than those observed upon binding to the isolated sites, so that the actual structure of the ternary complex likely differs significantly from the model shown in Figure 1C. It is worth noting that (1) the shape of the circular dichroism spectrum shows that distortion of the DNA from the B form is small, (2) the increase in the magnitude of the CD signal at 275 nm suggests a decrease in the DNA helix winding angle and an increase in the base pair twist angle (*73*), and (3) the increase in the absorbance signal could be indicative of base unstacking (*74*). From this evidence, we suggest that the change in DNA structure involves significant perturbation of base conformation but small backbone rearrangements because CD indicates that overall B conformation is maintained. We can visualize this as a small bubble without perturbing overall backbone conformation, but this primary event is crucial to helicase activity and subsequent assembly of the cellular DNA replication machinery. Our kinetic experiments show that there is a very small free energy barrier for this change in structure, because it takes place on the submillisecond time scale. From a functional point of view, simultaneous binding of two E2C-16 molecules to DBS may assist in the fast unwinding of the double helix at the start of replication fork progression (*8*, *28*, *29*, *75*), repress transcription trough displacement of the TATA binding protein and other regulatory proteins (*30*−*32*, *75*), and/or facilitate long-range interactions via DNA looping through its N-terminal domain (*34*, *35*).

Moreover, binding of the homologous E2C domains from HPV types 11, 16, and 18 to DBS provides us with an excellent model for studying how protein sequence divergence can modulate the thermodynamics of binding. The overall sequence identities for the DNA-binding domains are 54% for the 16/18 pair, 61% for the 16/11 pair, and 49% for the 11/18 pair. E2C−DNA binding is determined to a great degree by the side chains of the six highly conserved helix 1 residues involved in direct readout of the DNA bases (*18*), which are identical in the domains studied here. In agreement with this, the free energies of binding of the three proteins to BS1 and BS2 are very similar, differing by at most 0.5 kcal/mol (Table 1). This result contrasts with the variable K_{coop} for association with DBS, with E2C-11 and E2C-16 showing cooperative binding and E2C-18 showing additive binding (Table 2). Thus, the protein regions involved in cooperative binding must be variable among the three homologous proteins. Our cumulative folding and DNA binding studies on this domain (*36*) and recent NMR work show an unusual delocalized coupling among folding, dynamics, and DNA binding, which led us to conclude an "indirect readout from the protein side" (*52*), in agreement with the results presented in this work.

Binding cooperativity as described by K_{coop} is similar for E2C-11 and E2C-16. However, cooperativity is enthalpy-driven for E2C-11 and entropy-driven for E2C-16 (Figure 4). In addition, the associated spectroscopic changes are clearly different for the

two domains (Figure 5). In our view, depicting the binding of E2C-11 and E2C-16 to DBS as "similarly cooperative" would not be adequate. According to K_{coop}, E2C-18 binds to DBS in an additive, noncooperative manner. In the absence of other data, this would suggest that binding of the first protein molecule is indistinguishable from binding of the second one (Figure 4). Nevertheless, the lack of cooperativity for E2C-18 is due to compensating changes in enthalpy and entropy and is likely associated with sizable changes in the structure of the DNA that go beyond those expected for additive binding (Figure 5). Thus, we conclude that describing the binding of E2C-18 to DBS simply as noncooperative is not whole. Whereas changes in ΔG are less than 5%, differences in the enthalpic and entropic components are much larger and even of the opposite sign.

The activation of DNA replication is often linked to the transcription program. In the case of double-stranded DNA viruses, genome replication represses the expression of early proteins. This includes those participating directly in replication, such as HPV E2. Consequently, late protein expression is triggered, including the structural elements of the capsid, the shell that will transport the amplified viral DNA to new hosts (*3*, *4*). Our detailed structural and thermodynamic characterization of an important binding event for the coupling between replication and transcription (*20*) may aid the understanding of this process in papillomaviruses and in double-stranded DNA viruses in general.

ACKNOWLEDGMENT

We are grateful to Jesús Tejero for a discussion of kinetics data and Lori Frappier for helpful suggestions and comments on the manuscript.

SUPPORTING INFORMATION AVAILABLE

Raw CD and absorbance spectra for isolated and tandem DNA conformational changes, a scheme illustrating direct and reverse ITC titrations, and global fits to a two-independent binding site model. This material is available free of charge via the Internet at http://pubs.acs.org.

REFERENCES

1. Prado, F., and Aguilera, A. (2005) Impairment of replication fork progression mediates RNA polII transcription-associated recombination. *EMBO J. 24*, 1267–1276.
2. Liu, B., and Alberts, B. M. (1995) Head-on collision between a DNA replication apparatus and RNA polymerase transcription complex. *Science 267*, 1131–1137.
3. Flint, S. J., Enquist, L. W., Racaniello, V. R., and Skalka, A. M. (2008) Transcription strategies: DNA templates. In Principles of Virology, 3rd ed., pp 240−287, ASM Press, Washington, DC.
4. Flint, S. J., Enquist, L. W., Racaniello, V. R., and Skalka, A. M. (2008) Genome replication strategies: DNA viruses. In Principles of Virology, 3rd ed., pp 288−333, ASM Press, Washington, DC.
5. Kelly, T. J. (1988) SV40 DNA replication. *J. Biol. Chem. 263*, 17889–17892.
6. Komatsu, T., Ballestas, M. E., Barbera, A. J., Kelley-Clarke, B., and Kaye, K. M. (2004) KSHV LANA1 binds DNA as an oligomer and residues N-terminal to the oligomerization domain are essential for DNA binding, replication, and episome persistence. *Virology 319*, 225–236.
7. Polvino-Bodnar, M., and Schaffer, P. A. (1992) DNA binding activity is required for EBNA 1-dependent transcriptional activation and DNA replication. *Virology 187*, 591–603.
8. Chiang, C. M., Ustav, M., Stenlund, A., Ho, T. F., Broker, T. R., and Chow, L. T. (1992) Viral E1 and E2 proteins support replication of homologous and heterologous papillomaviral origins. *Proc. Natl. Acad. Sci. U.S.A. 89*, 5799–5803.
9. Cox, M., Ryder, K., Silver, S., and Tegtmeyer, P. (1988) The role of operator position in SV40 T-antigen-mediated repression. *Virology 167*, 293–295.
10. Lim, C., Sohn, H., Gwack, Y., and Choe, J. (2000) Latency-associated nuclear antigen of Kaposi's sarcoma-associated herpesvirus (human herpesvirus-8) binds ATF4/CREB2 and inhibits its transcriptional activation activity. *J. Gen. Virol. 81*, 2645–2652.
11. Thierry, F. (2009) Transcriptional regulation of the papillomavirus oncogenes by cellular and viral transcription factors in cervical carcinoma. *Virology 384*, 375–379.
12. Rawlins, D. R., Milman, G., Hayward, S. D., and Hayward, G. S. (1985) Sequence-specific DNA binding of the Epstein-Barr virus nuclear antigen (EBNA-1) to clustered sites in the plasmid maintenance region. *Cell 42*, 859–868.
13. Abbate, E. A., Voitenleitner, C., and Botchan, M. R. (2006) Structure of the papillomavirus DNA-tethering complex E2:Brd4 and a peptide that ablates HPV chromosomal association. *Mol. Cell 24*, 877–889.
14. Feeney, K. M., and Parish, J. L. (2009) Targeting mitotic chromosomes: A conserved mechanism to ensure viral genome persistence. *Proc. Biol. Sci. 276*, 1535–1544.
15. Titolo, S., Brault, K., Majewski, J., White, P. W., and Archambault, J. (2003) Characterization of the minimal DNA binding domain of the human papillomavirus e1 helicase: Fluorescence anisotropy studies and characterization of a dimerization-defective mutant protein. *J. Virol. 77*, 5178–5191.
16. Titolo, S., Welchner, E., White, P. W., and Archambault, J. (2003) Characterization of the DNA-binding properties of the origin-binding domain of simian virus 40 large T antigen by fluorescence anisotropy. *J. Virol. 77*, 5512–5518.
17. Wong, L. Y., and Wilson, A. C. (2005) Kaposi's sarcoma-associated herpesvirus latency-associated nuclear antigen induces a strong bend on binding to terminal repeat DNA. *J. Virol. 79*, 13829–13836.
18. Sanchez, I. E., Dellarole, M., Gaston, K., and de Prat Gay, G. (2008) Comprehensive comparison of the interaction of the E2 master regulator with its cognate target DNA sites in 73 human papillomavirus types by sequence statistics. *Nucleic Acids Res. 36*, 756–769.
19. Wyman, J., and Gill, S. J. (1990) Binding and linkage: Functional chemistry of biological macromolecules, UNSB, Mill Valley, CA.
20. Ptashne, M. (2004) A Genetic Switch-Phage Lambda Revisited, 3rd ed., Cold Spring Harbor Laboratory Press, Plainview, NY.
21. Tan, S., Leong, L. E., Walker, P. A., and Bernard, H. (1994) The human papillomavirus type 16 E2 transacription factor binds with low cooperativity to two flanking sites and represses the E6 promoter through displacement of Sp1 and TFIID. *J. Virol. 68*, 6411–6420.
22. Garber, A. C., Hu, J., and Renne, R. (2002) Latency-associated nuclear antigen (LANA) cooperatively binds to two sites within the terminal repeat, and both sites contribute to the ability of LANA to suppress transcription and to facilitate DNA replication. *J. Biol. Chem. 277*, 27401–27411.
23. Weisshart, K., Taneja, P., Jenne, A., Herbig, U., Simmons, D. T., and Fanning, E. (1999) Two regions of simian virus 40 T antigen determine cooperativity of double-hexamer assembly on the viral origin of DNA replication and promote hexamer interactions during bidirectional origin DNA unwinding. *J. Virol. 73*, 2201–2211.
24. Spalholz, B. A., Byrne, J. C., and Howley, P. M. (1988) Evidence for cooperativity between E2 binding sites in E2 trans-regulation of bovine papillomavirus type 1. *J. Virol. 62*, 3143–3150.
25. Summers, H., Barwell, J. A., Pfuetzner, R. A., Edwards, A. M., and Frappier, L. (1996) Cooperative assembly of EBNA1 on the Epstein-Barr virus latent origin of replication. *J. Virol. 70*, 1228–1231.
26. Bosch, F. X., Sanjosé, S., Castellsagué, X., Moreno, V., and Muñoz, N. (2006) Epimediology of Human Papillomavirus Infections and Associations with Cervical Cancer: New Opportunities for Prevention. In Papillomavirus Research: From Natural History to Vaccines and Beyond (Saveria Campo, M., Ed.) pp 19−40, Caisreir Academic Press, Wymondham, U.K.
27. Bernard, H. U., Burk, R. D., Chen, Z., van Doorslaer, K., Hausen, H. Z., and de Villiers, E. M. (2010) Classification of papillomaviruses (PVs) based on 189 PV types and proposal of taxonomic amendments. *Virology 401*, 70–79.
28. Lu, J. Z., Sun, Y. N., Rose, R. C., Bonnez, W., and McCance, D. J. (1993) Two E2 binding sites (E2BS) alone or one E2BS plus an A/T-rich region are minimal requirements for the replication of the human papillomavirus type 11 origin. *J. Virol. 67*, 7131–7139.
29. Sverdrup, F., and Khan, S. A. (1995) Two E2 binding sites alone are sufficient to function as the minimal origin of replication of human papillomavirus type 18 DNA. *J. Virol. 69*, 1319–1323.
30. Thierry, F., and Howley, P. M. (1991) Functional analysis of E2-mediated repression of the HPV18 P105 promoter. *New Biol. 3*, 90–100.
31. Tan, S. H., Gloss, B., and Bernard, H. U. (1992) During negative regulation of the human papillomavirus-16 E6 promoter, the viral E2

protein can displace Sp1 from a proximal promoter element. *Nucleic Acids Res. 20*, 251–256.
32. Dong, G., Broker, T. R., and Chow, L. T. (1994) Human papillomavirus type 11 E2 proteins repress the homologous E6 promoter by interfering with the binding of host transcription factors to adjacent elements. *J. Virol. 68*, 1115–1127.
33. Steger, G., and Corbach, S. (1997) Dose-dependent regulation of the early promoter of human papillomavirus type 18 by the viral E2 protein. *J. Virol. 71*, 50–58.
34. Hernandez-Ramon, E. E., Burns, J. E., Zhang, W., Walker, H. F., Allen, S., Antson, A. A., and Maitland, N. J. (2008) Dimerization of the human papillomavirus type 16 E2 N terminus results in DNA looping within the upstream regulatory region. *J. Virol. 82*, 4853–4861.
35. Sim, J., Ozgur, S., Lin, B. Y., Yu, J. H., Broker, T. R., Chow, L. T., and Griffith, J. (2008) Remodeling of the human papillomavirus type 11 replication origin into discrete nucleoprotein particles and looped structures by the E2 protein. *J. Mol. Biol. 375*, 1165–1177.
36. de Prat Gay, G., Gaston, K., and Cicero, D. O. (2008) The papillomavirus E2 DNA binding domain. *Front. Biosci. 13*, 6006–6021.
37. Hegde, R. S., Grossman, S. R., Laimins, L. A., and Sigler, P. B. (1992) Crystal structure at 1.7 Å of the bovine papillomavirus-1 E2 DNA-binding domain bound to its DNA target. *Nature 359*, 505–512.
38. Lima, L. M., and de Prat Gay, G. (1997) Conformational changes and stabilization induced by ligand binding in the DNA-binding domain of the E2 protein from human papillomavirus. *J. Biol. Chem. 272*, 19295–19303.
39. Mok, Y. K., Alonso, L. G., Lima, L. M., Bycroft, M., and de Prat Gay, G. (2000) Folding of a dimeric β-barrel: Residual structure in the urea denatured state of the human papillomavirus E2 DNA binding domain. *Protein Sci. 9*, 799–811.
40. Hegde, R. S. (2002) The papillomavirus E2 proteins: Structure, function, and biology. *Annu. Rev. Biophys. Biomol. Struct. 31*, 343–360.
41. de Prat Gay, G., Nadra, A. D., Corrales-Izquierdo, F. J., Alonso, L. G., Ferreiro, D. U., and Mok, Y. K. (2005) The folding mechanism of a dimeric β-barrel domain. *J. Mol. Biol. 351*, 672–682.
42. Bochkarev, A., Barwell, J. A., Pfuetzner, R. A., Bochkareva, E., Frappier, L., and Edwards, A. M. (1996) Crystal structure of the DNA-binding domain of the Epstein-Barr virus origin-binding protein, EBNA1, bound to DNA. *Cell 84*, 791–800.
43. Oddo, C., Freire, E., Frappier, L., and de Prat Gay, G. (2006) Mechanism of DNA recognition at a viral replication origin. *J. Biol. Chem. 281*, 26893–26903.
44. Kim, S. S., Tam, J. K., Wang, A. F., and Hegde, R. S. (2000) The structural basis of DNA target discrimination by papillomavirus E2 proteins. *J. Biol. Chem. 275*, 31245–31254.
45. Hooley, E., Fairweather, V., Clarke, A. R., Gaston, K., and Brady, R. L. (2006) The recognition of local DNA conformation by the human papillomavirus type 6 E2 protein. *Nucleic Acids Res. 34*, 3897–3908.
46. Ferreiro, D. U., Dellarole, M., Nadra, A. D., and de Prat Gay, G. (2005) Free energy contributions to direct readout of a DNA sequence. *J. Biol. Chem. 280*, 32480–32484.
47. Ferreiro, D. U., and de Prat Gay, G. (2003) A protein-DNA binding mechanism proceeds through multi-state or two-state parallel pathways. *J. Mol. Biol. 331*, 89–99.
48. Ferreiro, D. U., Sanchez, I. E., and de Prat Gay, G. (2008) Transition state for protein-DNA recognition. *Proc. Natl. Acad. Sci. U.S.A. 105*, 10797–10802.
49. Sanchez, I. E., Ferreiro, D. U., Dellarole, M., and de Prat Gay, G. (2010) Experimental snapshots of a protein-DNA binding landscape. *Proc. Natl. Acad. Sci. U.S.A. 107*, 7751–7756.
50. Nadra, A. D., Eliseo, T., Mok, Y. K., Almeida, C. L., Bycroft, M., Paci, M., de Prat Gay, G., and Cicero, D. O. (2004) Solution structure of the HPV-16 E2 DNA binding domain, a transcriptional regulator with a dimeric β-barrel fold. *J. Biomol. NMR 30*, 211–214.
51. Dellarole, M., Sanchez, I. E., Freire, E., and de Prat Gay, G. (2007) Increased Stability and DNA Site Discrimination of "Single Chain" Variants of the Dimeric β-Barrel DNA Binding Domain of the Human Papillomavirus E2 Transcriptional Regulator. *Biochemistry 46*, 12441–12450.
52. Eliseo, T., Sanchez, I. E., Nadra, A. D., Dellarole, M., Paci, M., de Prat Gay, G., and Cicero, D. O. (2009) Indirect DNA readout on the protein side: Coupling between histidine protonation, global structural cooperativity, dynamics, and DNA binding of the human papillomavirus type 16 E2C domain. *J. Mol. Biol. 388*, 327–344.
53. Gray, D. M., Hung, S. H., and Johnson, K. H. (1995) Absorption and circular dichroism spectroscopy of nucleic acid duplexes and triplexes. *Methods Enzymol. 246*, 19–34.
54. Ferreiro, D. U., Lima, L. M., Nadra, A. D., Alonso, L. G., Goldbaum, F. A., and de Prat Gay, G. (2000) Distinctive cognate sequence discrimination, bound DNA conformation, and binding modes in the E2 C-terminal domains from prototype human and bovine papillomaviruses. *Biochemistry 39*, 14692–14701.
55. Mok, Y. K., de Prat Gay, G., Butler, P. J., and Bycroft, M. (1996) Equilibrium dissociation and unfolding of the dimeric human papillomavirus strain-16 E2 DNA-binding domain. *Protein Sci. 5*, 310–319.
56. Alexander, K. A., and Phelps, W. C. (1996) A fluorescence anisotropy study of DNA binding by HPV-11 E2C protein: A hierarchy of E2-binding sites. *Biochemistry 35*, 9864–9872.
57. Schneider, T. D., and Stephens, R. M. (1990) Sequence logos: A new way to display consensus sequences. *Nucleic Acids Res. 18*, 6097–6100.
58. Crooks, G. E., Hon, G., Chandonia, J. M., and Brenner, S. E. (2004) WebLogo: A sequence logo generator. *Genome Res. 14*, 1188–1190.
59. Büchen-Osmond, C. (2003) The Universal Virus Database ICTVdB. *Comput. Sci. Eng. 5* (3), 16–25.
60. Clamp, M., Cuff, J., Searle, S. M., and Barton, G. J. (2004) The Jalview Java alignment editor. *Bioinformatics 20*, 426–427.
61. Wiseman, T., Williston, S., Brandts, J. F., and Lin, L. N. (1989) Rapid measurement of binding constants and heats of binding using a new titration calorimeter. *Anal. Biochem. 179*, 131–137.
62. Houtman, J. C., Brown, P. H., Bowden, B., Yamaguchi, H., Appella, E., Samelson, L. E., and Schuck, P. (2007) Studying multisite binary and ternary protein interactions by global analysis of isothermal titration calorimetry data in SEDPHAT: Application to adaptor protein complexes in cell signaling. *Protein Sci. 16*, 30–42.
63. Gray, D. (1996) Circular Dichroism of Protein Nucleic Acid Interactions. In Circular Dichroism and the Conformational Analysis of Biomolecules (Fasman, G., Ed.) Plenum Press, New York.
64. Baase, W. A., and Johnson, W. C., Jr. (1979) Circular dichroism and DNA secondary structure. *Nucleic Acids Res. 6*, 797–814.
65. Bains, G., and Freire, E. (1991) Calorimetric determination of cooperative interactions in high affinity binding processes. *Anal. Biochem. 192*, 203–206.
66. Freire, E., Schon, A., and Velazquez-Campoy, A. (2009) Isothermal titration calorimetry: General formalism using binding polynomials. *Methods Enzymol. 455*, 127–155.
67. Brown, A. (2009) Analysis of cooperativity by isothermal titration calorimetry. *Int. J. Mol. Sci. 10*, 3457–3477.
68. Schumacher, M. A., Miller, M. C., Grkovic, S., Brown, M. H., Skurray, R. A., and Brennan, R. G. (2002) Structural basis for cooperative DNA binding by two dimers of the multidrug-binding protein QacR. *EMBO J. 21*, 1210–1218.
69. Lacal, J., Guazzaroni, M. E., Gutierrez-del-Arroyo, P., Busch, A., Velez, M., Krell, T., and Ramos, J. L. (2008) Two levels of cooperativeness in the binding of TodT to the tod operon promoter. *J. Mol. Biol. 384*, 1037–1047.
70. Dragan, A. I., Carrillo, R., Gerasimova, T. I., and Privalov, P. L. (2008) Assembling the human IFN-β enhanceosome in solution. *J. Mol. Biol. 384*, 335–348.
71. Weinberg, R. L., Veprintsev, D. B., and Fersht, A. R. (2004) Cooperative binding of tetrameric p53 to DNA. *J. Mol. Biol. 341*, 1145–1159.
72. Thain, A., Webster, K., Emery, D., Clarke, A. R., and Gaston, K. (1997) DNA binding and bending by the human papillomavirus type 16 E2 protein. Recognition of an extended binding site. *J. Biol. Chem. 272*, 8236–8242.
73. Johnson, B. B., Dahl, K. S., Tinoco, I., Jr., Ivanov, V. I., and Zhurkin, V. B. (1981) Correlations between deoxyribonucleic acid structural parameters and calculated circular dichroism spectra. *Biochemistry 20*, 73–78.
74. Di Pietro, S. M., Centeno, J. M., Cerutti, M. L., Lodeiro, M. F., Ferreiro, D. U., Alonso, L. G., Schwarz, F. P., Goldbaum, F. A., and de Prat Gay, G. (2003) Specific antibody-DNA interaction: A novel strategy for tight DNA recognition. *Biochemistry 42*, 6218–6227.
75. Alexandrov, B. S., Gelev, V., Bishop, A. R., Usheva, A., and Rasmussen, K. O. (2010) DNA Breathing Dynamics in the Presence of a Terahertz Field. *Phys. Lett. A 374*, 1214.